

Steering Action-aware Adaptive Cruise Control for Teleoperated Driving

Andreas Schimpe, Domagoj Majstorovic and Frank Diermeyer

Abstract—In this paper, a steering action-aware Adaptive Cruise Control (ACC) approach for teleoperated road vehicles is proposed. In order to keep the vehicle in a safe state, the ACC approach can override the human operator’s velocity control commands. The safe state is defined as a state from which the vehicle can be stopped safely, no matter which steering actions are applied by the operator. This is achieved by first sampling various potential future trajectories. In a second stage, assuming the trajectory with the highest risk, a safe and comfortable velocity profile is optimized. This yields a safe velocity control command for the vehicle. In simulations, the characteristics of the approach are compared to a Model Predictive Control-based approach that is capable of overriding both, the commanded steering angle as well as the velocity. Furthermore, in teleoperation experiments with a 1:10-scale vehicle testbed, it is demonstrated that the proposed ACC approach keeps the vehicle safe, even if the control commands from the operator would have resulted in a collision.

I. INTRODUCTION

The technology of road vehicle teleoperation, i.e., Teleoperated Driving (ToD) holds the promise to achieve truly driverless automated vehicles (AVs) [1, 2]. It is assumed that the AV is capable of fully automated driving (AD). However, at some point, the function may reach a constraint of its operational design domain, e.g., an intersection that is controlled by a policeman. Resolving such a traffic situation may not yet be covered by the AD function. Instead, the vehicle comes to a stop and requests support from a remote vehicle control center (VCoC). From there, a human operator connects to the vehicle via mobile networks. Transmission of sensor data, in particular vehicle state information and video streams, from the vehicle to the VCoC is initiated. There, the data are displayed to the operator, giving him an understanding of the vehicle surroundings. Based on this, the operator is able to generate control commands, which are transmitted back to the vehicle for execution. ToD comes with challenges. Data, as perceived by an operator, are subject to latency due to processing and the transmission via a mobile network [3], which also yields the risk of an unstable connection [4]. Furthermore, due to various reasons, the situation awareness (SA) of an operator in the VCoC may be lower than the SA of a driver in the vehicle. Frequently described issues are the “out-of-the-loop-syndrome,” having to deal with an unfamiliar traffic situation at short notice, or an operator’s missing sense of embodiment, i.e., an adequate feeling for the actual motion of the controlled vehicle [5].

The authors are with the Institute for Automotive Technology at the Technical University of Munich (TUM), 85748 Garching bei München, Germany. andreas.schimpe@tum.de

A. Vehicle Teleoperation Concepts

Remote assistance or control concepts can be designed in different ways in order to resolve the various fail cases of a complex AD function. For instance, the concept in [6] aims at enabling remote assistance for tasks related to perception. Interactive path planning approaches [7, 8] assume a functional perception module and support the AD function at the decision making layer. While the human operator takes over the legal responsibility for this decision, it is the responsibility of the AD function to ensure the safety of the vehicle during execution.

At the lowest layer, remote assistance at the control layer is possible through direct teleoperation, i.e., an operator is controlling the vehicle at stabilization level. Through a conventional control interface, consisting of a steering wheel and pedals, the operator generates lateral and longitudinal motion control commands, which are sent to the vehicle actuators via the mobile network. This control concept makes minimal to no assumptions about the operation of AD function modules. However, especially due to the previously described challenges of ToD, it also yields the greatest workload for the operator, who essentially takes over all aforementioned tasks of the AD function, namely correct perception, legal decision making as well as the safe motion of the vehicle. In the presented work, shared control is seen as a vehicle teleoperation concept that keeps the convenience of a conventional control interface, but supports the operator in ensuring the safety of the vehicle.

B. Uncoupled Shared Control for Vehicle Teleoperation

Shared control is a case of human-machine interaction. In a shared control system, a human and an automation component are collaborating in performing a task, e.g., controlling a vehicle. In this context, as introduced in [9], it can be distinguished between coupled and uncoupled shared control designs. In the coupled case, the partners, human and machine, are acting on mechanically coupled actuators. Authority is held by the partner applying the greater force. In contrast to this, uncoupled shared control is applicable in a drive-by-wire system. The automation is receiving the control actions from the human as a reference and can override if deemed necessary, e.g., in order to avoid an imminent collision of the controlled vehicle. Being the focus of the approach proposed in this paper, this capability makes uncoupled shared control in particular of great interest for the use case of vehicle teleoperation [10].

C. Related Work

Various uncoupled shared control designs have been proposed. Several approaches assist the human driver or operator in ensuring safe lateral motion control of teleoperated vehicles [11, 12] or experimental drive-by-wire vehicles operated at high speed [13]. It is obvious that those approaches can no longer ensure vehicle safety if a collision can only be avoided through braking. In consequence, multiple approaches address this issue, given the capability of also overriding the human’s longitudinal control command, i.e., desired velocity or acceleration. This has proven to effectively improve vehicle safety in environments with static [14] and dynamic obstacles [15, 16].

Throughout the years, cruise control, which only decouples longitudinal control from the driver, has been designed for different tasks and purposes. For instance, predictive cruise control approaches aim at improving fuel economy through the use of upcoming traffic signal information [17] or high-definition maps [18]. Adaptive Cruise Control (ACC) designs have the objective to keep the controlled vehicle safe, while it is performing lane keeping and car following. Some designs specifically address safety in the case of unexpected behavior of surrounding vehicles, e.g., cut-in situations [19] or full braking of the preceding vehicle [20]. Furthermore, cooperative ACC, the controlled vehicle being connected to the preceding vehicle, has been shown to enable smaller safety distances and improve traffic-flow stability [21]. The ACC approach in [22], developed for ToD tasks, considers urban scenarios involving cross traffic.

Classical ACC approaches assume that the controlled vehicle is performing lane keeping. Unforeseen lateral maneuvers, e.g., sudden lane changes or turns in urban scenarios, are not considered and thus safety would not be ensured. For the challenging task of ToD, steering actions from the human operator may not be safe at all times.

D. Contributions

In this paper, a steering action-aware ACC approach for ToD is proposed. As an active safety system, the approach can override the human operator’s velocity control commands. As visualized in Fig. 1, it consists of two stages. First, various future steering actions are evaluated. Second, a safe velocity profile is optimized. In simulations, the characteristics of the ACC approach are compared to a baseline shared controller, capable of also overriding the commanded steering angle. Furthermore, the approach is validated in experiments with an actual operator, teleoperating a 1:10-scale vehicle testbed.

II. APPROACH

The procedure, corresponding to the stages of the steering action-aware ACC approach, visualized in Fig. 1, is given in Alg. 1. From the current vehicle state with the steering angle δ_{curr} and velocity v_{curr} , the `TreePlanner` samples various future steering actions in line 2. In line 3, the generated trajectories are checked for collisions with the list of obstacles O . Thereby, the collision-free, i.e., the safe progress in meters along each trajectory is computed.

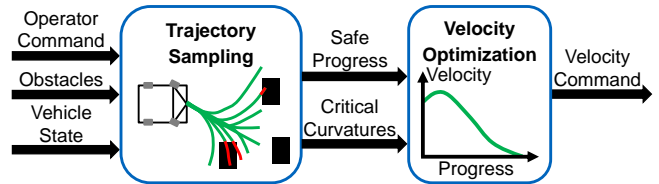


Fig. 1: Stages of Steering Action-aware ACC Approach.

Algorithm 1 Compute Adaptive Cruise Control Command

```

1: procedure ComputeCommand( $\delta_{\text{curr}}, v_{\text{curr}}, a_{\text{curr}}, v_{\text{des}}, O$ )
2:   TreePlanner.GenerateTrajectoriesFrom( $\delta_{\text{curr}}, v_{\text{curr}}$ )
3:   TreePlanner.CheckForCollisionsWith( $O$ )
4:    $s_{\text{safe}} \leftarrow$  TreePlanner.GetGlobalSafeProgress()
5:    $\kappa_{\text{crit}}^N \leftarrow$  TreePlanner.GetCriticalCurvatureProfile()
6:    $v_{\text{opt}} \leftarrow$  VelocityOptimizer.solve( $v_{\text{curr}}, a_{\text{curr}}, v_{\text{des}}, s_{\text{safe}}, \kappa_{\text{crit}}^N$ )
7:   return  $v_{\text{opt}}(1)$ 
8: end procedure

```

The minimal safe progress from all trajectories, i.e., the global safe progress s_{safe} is taken in line 4. Also from the `TreePlanner`, the critical curvature profile κ_{crit}^N is taken in line 5. Here and throughout the remainder of this section, superscript N denotes the course of the corresponding variable over the planning horizon, discretized in N steps. In line 6, from the current velocity and acceleration a_{curr} of the vehicle, the `VelocityOptimizer` solves for a velocity profile, taking into account the desired velocity of the human operator v_{des} , the global safe progress and the critical curvature profile. From this profile, the entry at time instant 1 is returned from the algorithm in line 7 as the velocity command to be executed by the vehicle.

In the remainder of this section, more details on the above steps are provided. For brevity, they are summarized as *A. Trajectory Sampling* (lines 2 to 5), yielding the global safe progress and the critical curvature profile, and *B. Velocity Optimization* (lines 6 and 7), computing the safe velocity control command for the vehicle.

A. Trajectory Sampling

At each sampling instant of the controller, a trajectory tree, a set of trajectories of time horizon T_H , discretized in N steps by the sampling time t_s , is generated. Assuming only moderate speeds during vehicle teleoperation, the well-known kinematic bicycle model [23] is used in order to plan the trajectories. For this, the system states are $z = [x, y, \theta, \delta, v]^T$, with the center of mass (CoM) position of the vehicle in x and y , the heading θ , the steering angle δ and the velocity v . The inputs to the system are $u = [\dot{\delta}, a]^T$, with the steering angle rate $\dot{\delta}$ and the acceleration a .

1) *Trajectory Generation*: As pointed out earlier, the ACC evaluates various future steering actions commanded by the human operator within the planning horizon. The trajectory states are computed using the Forward Euler method, given by $z_{n+1} = z_n + t_s \dot{z}_n$ for $n = 0, 1, \dots, N-1$.

The trajectories of the tree are planned by varying the steering angle rate in M steps within a steering angle rate range $[-\dot{\delta}_{\text{max}}, \dot{\delta}_{\text{max}}]$, with an assumed maximum steering

angle rate $\dot{\delta}_{\max}$. All trajectories plan to brake the vehicle to a standstill by applying a constant deceleration $a_{\text{stop}} = -v_{\text{curr}}/T_H$. In summary, the M trajectories of the tree are planned by applying constant control inputs $u_m = [\dot{\delta}_m, a_{\text{stop}}]^T$ with $\dot{\delta}_m = -\dot{\delta}_{\max} + 2\dot{\delta}_{\max}(m-1)/(M-1)$ for $m = 1, 2, \dots, M$. In Fig. 2, with parameters from a passenger vehicle, a snapshot of generated trajectories is visualized. In Fig. 2a, the trajectories are shown in the xy plane. Fig. 2b plots the velocities and steering angles over the trajectory progress.

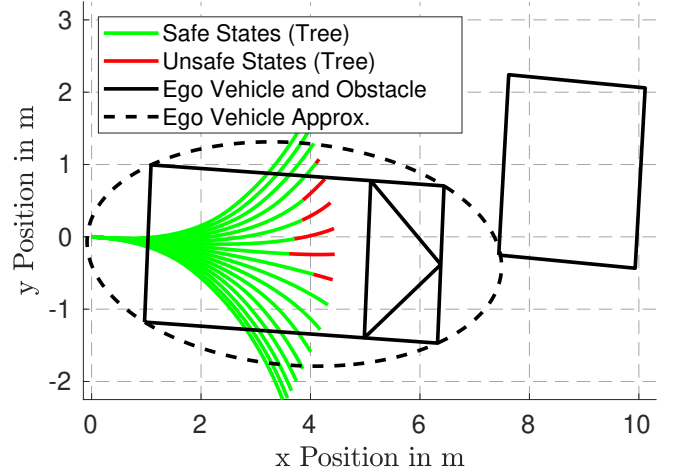
2) *Collision Checking and Assessment of Global Safe Progress*: To assess the global safe progress from the current vehicle state, all states, i.e., discretization points from the generated trajectories are checked for collisions with the list of surrounding obstacles O . When iterating, the safe progress in meters along each trajectory is accumulated until (if at all) a state with a collision is detected. For performing the collision checks, the obstacles are transformed into the vehicle coordinate frame, located at the CoM. In Fig. 2, safe and unsafe states are plotted. In addition, in Fig. 2a, the dimensions of an obstacle and the vehicle, located at the first state for which a collision is detected, are shown. As visualized, collision checks are performed by approximating the rectangular vehicle as an ellipse and checking whether the edge or corner points of the obstacle lie within. Finally, the safe progress values from all trajectories are compared, and the minimum, i.e., the global safe progress s_{safe} is forwarded to the velocity optimization procedure.

Planning trajectories with constant steering rates does not evaluate all possible operator steering actions. Instead, it would be expected that the planner varies the steering rate along the trajectories. However, while this would increase the density of the trajectory tree, it has been found that the resulting global safe progress and the critical curvature profile, described next, are essentially not affected by this. In consequence, it is deemed sufficient to plan with constant steering rates.

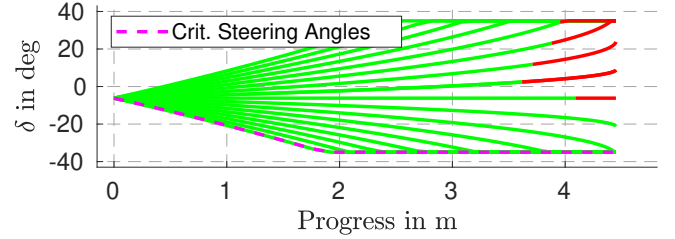
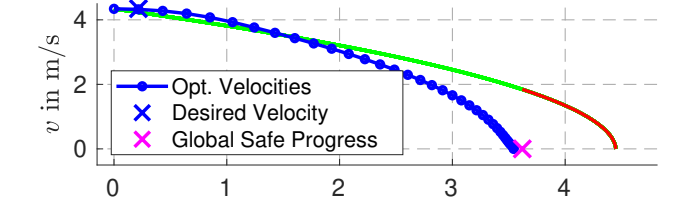
3) *Computation of Critical Curvature Profile*: To account for lateral acceleration constraints in the velocity optimization, a critical curvature profile κ_{crit}^N is computed by the trajectory tree planner. This profile stems from the steering angle profile that reaches the maximum steering angle δ_{\max} the earliest. In short, it is generated by applying the constant steering angle rate $\dot{\delta}_{\text{crit}} = \text{sign}(\delta_{\text{curr}})\dot{\delta}_{\max}$ until the maximum steering angle is reached. Exemplarily, this is shown in the steering angle plot in Fig. 2b. Finally, from each steering angle, the corresponding curvature is computed from the kinematic bicycle model equations.

B. Velocity Optimization

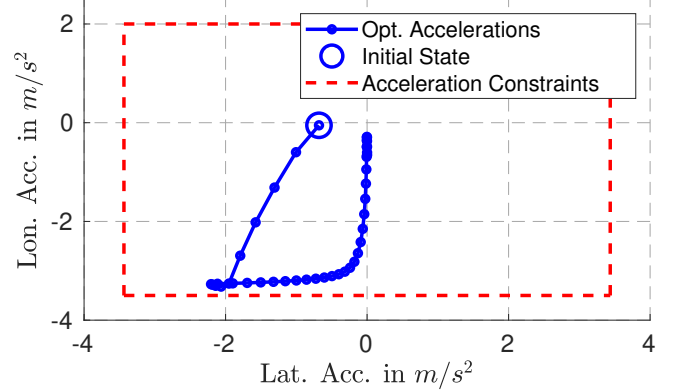
After the trajectory sampling, the velocity profile is optimized in a Model Predictive Control (MPC) fashion. On the one hand, the objective is to reach the velocity desired by the human operator. On the other, the velocity profile should brake the vehicle to a standstill, while satisfying safety and comfort constraints.



(a) Generated trajectory tree in the xy plane. Safe and unsafe states are depicted. An obstacle and the controlled vehicle, located at the first colliding state with its elliptical approximation, are shown.



(b) Profiles of velocities (top) and steering angles (bottom) over progress along trajectories in the tree. In the velocity plot, the desired velocity and the global safe progress are marked. Furthermore, the solution of the velocity optimization is shown. In the steering angle plot, the profile of critical steering angles is shown as well.



(c) Acceleration diagram. With the initial state being marked, the acceleration profile, resulting from the velocity optimization, is plotted. In addition, the acceleration constraints are shown.

Fig. 2: Controller computations at one sampling instant.

The optimization problem, also discretized in N time steps of length t_s , is given by

$$\min w_{v,\text{des}} (v_1 - v_{\text{des}})^2 + w_{v,\text{term}} v_N^2 + J_s \quad (1a)$$

subject to

$$s_0 = 0 \text{ m}, v_0 = v_{\text{curr}}, a_0 = a_{\text{curr}}, \quad (1b)$$

$$s_{n+1} = s_n + t_s v_n, v_{n+1} = v_n + t_s a_n, a_{n+1} = a_n + t_s j_n, \quad (1c)$$

$$s_{n+1} \leq s_{\text{safe}}, \quad (1d)$$

$$-a_{\text{lat,max}} \leq \kappa_{\text{crit},n+1} v_{n+1}^2 \leq a_{\text{lat,max}}, \quad (1e)$$

$$a_{\text{min}} - s_{l a,n+1} \leq a_{n+1} \leq a_{\text{max}} + s_{u a,n+1}, \quad (1f)$$

$$-j_{\text{max}} - s_{l j,n} \leq j_n \leq j_{\text{max}} + s_{u j,n}, \quad (1g)$$

for $n = 0, 1, \dots, N-1$.

In the cost function (1a), weighted by $w_{v,\text{des}}$, the primary objective is to reach the desired velocity v_{des} at the first predicted instant of the horizon v_1 . Heavily weighted by $w_{v,\text{term}}$, the terminal velocity v_N should reach 0 m/s. The system is modelled as a point mass with system states $[s, v, a]^T$ and jerk j as control input. The initial state condition and the model equations are given in (1b) and (1c), respectively. Through (1d) and (1e), progress and lateral acceleration of the vehicle are constrained to not exceed the global safe progress s_{safe} and the lateral acceleration limit $a_{\text{lat,max}}$. Being results from the trajectory sampling stage, s_{safe} and the critical curvature profile κ_{crit}^N are parameters that are updated at each sampling instant of the controller. Finally, through (1f) and (1g), acceleration and jerk are constrained. To cope with noise in the vehicle feedback, and yet achieve the feasibility of the optimization problem, these constraints are made soft. This is achieved by introducing the slack variables $s_{(\cdot,\cdot)}$, which are penalized in the cost function term J_s .

Exemplarily, for the sampling instant visualized in Fig. 2, the optimized velocity and acceleration profiles are shown in the velocity plot of Fig. 2b and the acceleration diagram in Fig. 2c, respectively. Although not all trajectories of the tree are collision-free, the velocity profile can be planned, maintaining the desired velocity and reaching a standstill at the global safe progress. Neither the longitudinal nor the lateral accelerations exceed the imposed constraints.

III. SIMULATION RESULTS

The proposed ACC approach has been validated in the software framework for ToD, introduced in [24]. The characteristics of the approach are compared to those of a baseline shared control approach, capable of also overriding the steering actions from the human operator.

A. Simulation Setup

In the presented simulations, the steering actions from the human operator are simulated through a feedback linearization-based path tracking controller [25], following a straight reference path with a constant desired velocity of 5 m/s. The scenario, visualized in the xy plane in Fig. 3a, consists of five static obstacles. With decreasing displacement in the y direction, obstacles ①-④ are placed alternately left and right of the operator reference path. The wider obstacle ⑤ is centered on the reference.

The baseline shared control approach is based on MPC. Closely following the formulation presented in [16], it is capable of velocity and steering intervention. Early in the prediction horizon, the MPC aims to track the current operator control command. Obstacle avoidance constraints lead to interventions of the MPC if the operator's control actions would not be collision-free.

Both control approaches, ACC and MPC, are running at 20 Hz, a rate easily achieved, given average computation times per sampling instant of less than 10 ms. All prediction horizons, those from the trajectory tree, velocity optimization and MPC, are set to $T_H = 2$ s, discretized in $N = 40$ steps, yielding a sampling time of $t_s = 50$ ms.

The optimization problems of the velocity optimization and the MPC are solved using `acados` [26], a software package for fast embedded optimization of nonlinear MPC formulations. Internally, `acados` implements a Sequential Quadratic Programming (SQP) algorithm, in which QP subproblems are treated by an efficient QP solver. In this work, the QP solver of choice is `HPiPM` [27].

B. Results

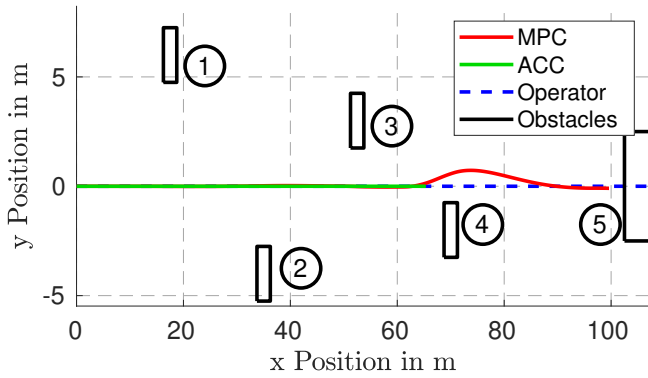
The performance of the two different shared control approaches in the given scenario is shown in Fig. 3. In Fig. 3a, the driven trajectories are shown in the xy plane. Together with the human operator references, the vehicle velocities and steering angles are plotted over time in Fig. 3b.

As shown, the ACC tracks the reference velocity, when passing obstacle ①. In proximity to the obstacles ② and ③, as a smaller s_{safe} is computed, the velocity is reduced to approximately 4 m/s and 2 m/s, respectively. Obstacle ④ could not be passed without steering. In consequence, at approximately $x = 65$ m, the ACC brings the vehicle to a standstill. A video of the ACC simulation is available¹.

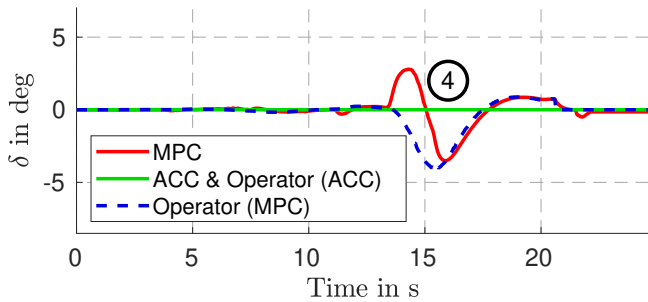
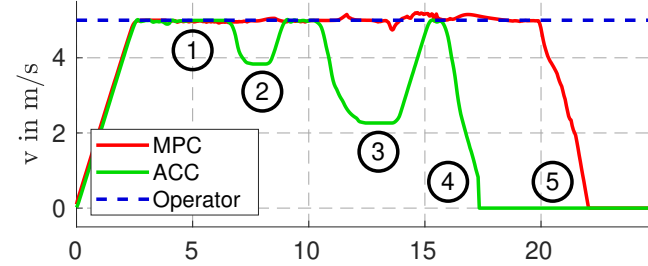
In contrast, the MPC tracks the reference velocity and steering angle consistently when obstacles ① to ③ are passed. Obstacle ④ is avoided through a minor steering intervention, i.e., deviation from the operator reference. In order to pass obstacle ⑤, the steering intervention would need to be much greater. Instead, at approximately $x = 100$ m, the MPC brings the vehicle to a standstill as well. A video of the MPC simulation is available².

¹Video of ACC simulation: <https://youtu.be/yFzSiwtUtq4>

²Video of MPC simulation: <https://youtu.be/vz8slCFW140>



(a) Trajectories in the xy plane for the two control approaches. In addition, the operator reference and obstacles are shown.



(b) Courses of the actual and desired velocities (top) and steering angles (bottom) over time for the two control approaches.

Fig. 3: Comparison of ACC and MPC approaches.

IV. EXPERIMENTAL RESULTS

The ACC approach has also been validated experimentally with a 1:10-scale vehicle testbed [28]. The setup of the experiment is shown in Fig. 5. The vehicle was teleoperated from the VCoC through a course with several obstacles, which were detected by clustering the returns from the onboard 2D lidar sensor. Video streams of the onboard stereo camera from the vehicle as well as control commands from the human operator were transmitted via wireless LAN.

The course of the desired and actual velocities as well as steering angles are plotted in Fig. 4. The controller keeps the vehicle in a safe state, reducing the velocity in proximity to the encountered obstacles. At the time of approximately 25 s, the operator's steering actions were no longer collision-free. In consequence, the vehicle is brought to a standstill by the ACC. A video of the experiment is available³.

³Video of teleoperation experiment: <https://youtu.be/dumicX-PZow>

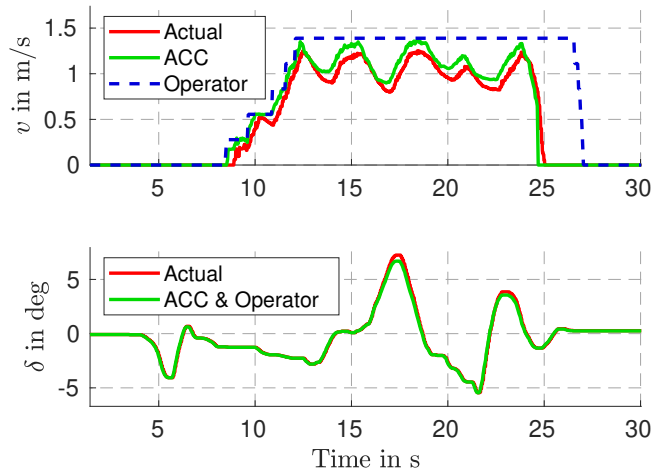


Fig. 4: Courses of the velocities (top) and steering angles (bottom) desired by the operator, commanded by the ACC and actually executed by the vehicle over time during the teleoperation experiment with the 1:10-scale vehicle testbed.

V. CONCLUSION

In this paper, a steering action-aware ACC approach for teleoperated road vehicles has been proposed. Without the need to override the human operator's steering actions, it was demonstrated that the approach can keep the vehicle in a safe state, i.e., the vehicle can be stopped safely at all times. In simulations, the characteristics of the ACC approach were compared to those of a baseline shared control approach based on MPC, capable of also overriding the operator's steering actions. Finally, the ACC was validated in a teleoperation experiment with a 1:10-scale vehicle testbed.

In future work, the trajectory sampling of the ACC will be extended to account for dynamic obstacles. Furthermore, the shared control framework will be complemented by visual and haptic feedback in order to establish an advanced bilateral communication channel between the shared controllers and the human operator. The effects on vehicle operability of the approaches will then be assessed in a human subjects study.

ACKNOWLEDGEMENTS

Andreas Schimpe developed and implemented the shared control approaches. In fruitful discussions, Domagoj Majstorovic contributed to their refinement. The experiments with the 1:10-scale vehicle testbed were supported by Tanay Dwivedi and Florian Sauerbeck. Frank Diermeyer contributed to the essential concept of the research project. He revised the manuscript critically for important intellectual content and gave final approval of the version to be published. He agrees with all aspects of the work. The research was partially funded by the European Union (EU) under RIA grant No. 825050, and through basic research funds from the Institute for Automotive Technology.

REFERENCES

- [1] J. M. Georg, J. Feiler, F. Diermeyer, and M. Lienkamp, "Teleoperated Driving, a Key Technology for Automated Driving? Comparison of Actual Test Drives with a Head Mounted Display and Conventional

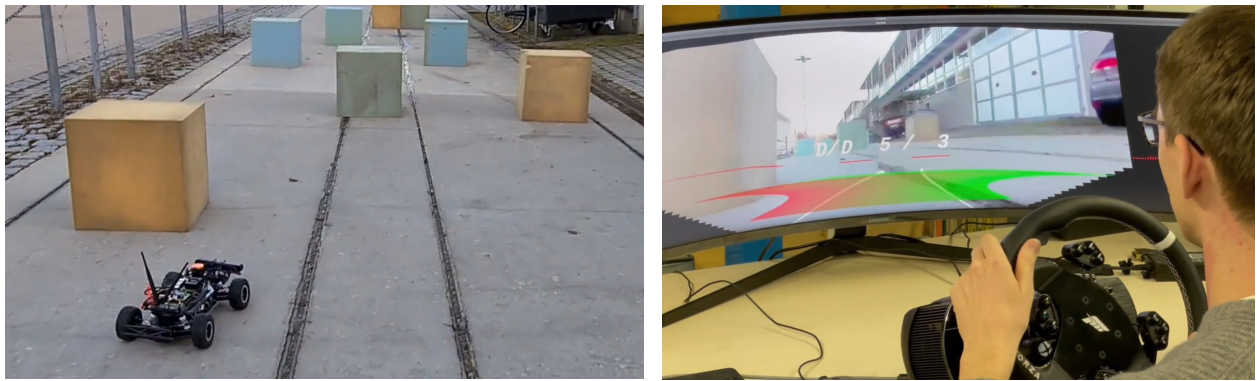


Fig. 5: Setup of the teleoperation experiment with the 1:10-scale vehicle testbed. The left picture depicts the vehicle and foam cubes used as obstacles. On the right picture, the VCoC setup is shown with the operator, the monitor with live videos transmitted from the vehicle, and the steering wheel used to generate the remote control commands.

- Monitors*," in *IEEE Conference on Intelligent Transportation Systems (ITSC)*. IEEE, 2018, pp. 3403–3408.
- [2] S. Neumeier, N. Gay, C. Dannheim, and C. Facchi, "On the way to autonomous vehicles teleoperated driving," *AmE 2018: Automotive meets Electronics - 9. GMM-Fachtagung*, pp. 49–54, 2018.
 - [3] J.-M. Georg, J. Feiler, S. Hoffmann, and F. Diermeyer, "Sensor and Actuator Latency during Teleoperation of Automated Vehicles," in *2020 IEEE Intelligent Vehicles Symposium (IV)*. IEEE, 2020, pp. 760–766.
 - [4] S. Hoffmann and F. Diermeyer, "Systems-theoretic Safety Assessment of Teleoperated Road Vehicles," in *Proceedings of the 7th International Conference on Vehicle Technology and Intelligent Transport Systems*. SCITEPRESS - Science and Technology Publications, 2021, pp. 446–456.
 - [5] C. Mutzenich, S. Durant, S. Helman, and P. Dalton, "Updating our understanding of situation awareness in relation to remote operators of autonomous vehicles," *Cognitive Research: Principles and Implications*, vol. 6, no. 1, p. 9, 2021.
 - [6] J. Feiler and F. Diermeyer, "The Perception Modification Concept to Free the Path of An Automated Vehicle Remotely," in *Proceedings of the 7th International Conference on Vehicle Technology and Intelligent Transport Systems*. SCITEPRESS - Science and Technology Publications, 2021, pp. 405–412.
 - [7] A. Hosseini, T. Wiedemann, and M. Lienkamp, "Interactive path planning for teleoperated road vehicles in urban environments," in *17th International IEEE Conference on Intelligent Transportation Systems (ITSC)*. IEEE, 2014, pp. 400–405.
 - [8] D. Schitz, S. Bao, D. Rieth, and H. Aschemann, "Shared Autonomy for Teleoperated Driving: A Real-Time Interactive Path Planning Approach," in *2021 IEEE International Conference on Robotics and Automation (ICRA)*. IEEE, 2021, pp. 999–1004.
 - [9] M. Marcano, S. Diaz, J. Perez, and E. Irigoyen, "A Review of Shared Control for Automated Vehicles: Theory and Applications," *IEEE Transactions on Human-Machine Systems*, vol. 50, no. 6, pp. 475–491, 2020.
 - [10] D. Majstorovic, S. Hoffmann, F. Pfab, A. Schimpe, M.-M. Wolf, and F. Diermeyer, "Survey on Teleoperation Concepts for Automated Vehicles," in *2022 IEEE International Conference on Systems, Man and Cybernetics (SMC)*, accepted, 2022.
 - [11] S. J. Anderson, S. C. Peters, T. E. Pilutti, and K. Iagnemma, "An optimal-control-based framework for trajectory planning, threat assessment, and semi-autonomous control of passenger vehicles in hazard avoidance scenarios," *International Journal of Vehicle Autonomous Systems*, vol. 8, no. 2/3/4, p. 190, 2010.
 - [12] A. Schimpe and F. Diermeyer, "Steer with Me: A Predictive, Potential Field-Based Control Approach for Semi-Autonomous, Teleoperated Road Vehicles," in *2020 IEEE 23rd International Conference on Intelligent Transportation Systems (ITSC)*. IEEE, 2020, pp. 1–6.
 - [13] S. M. Erlen, S. Fujita, and J. C. Gerdes, "Shared Steering Control Using Safe Envelopes for Obstacle Avoidance and Vehicle Stability," *IEEE Transactions on Intelligent Transportation Systems*, vol. 17, no. 2, pp. 441–451, 2016.
 - [14] J. Storms, K. Chen, and D. Tilbury, "A shared control method for obstacle avoidance with mobile robots and its interaction with communication delay," *The International Journal of Robotics Research*, vol. 36, no. 5-7, pp. 820–839, 2017.
 - [15] W. Schwarting, J. Alonso-Mora, L. Paull, S. Karaman, and D. Rus, "Safe Nonlinear Trajectory Generation for Parallel Autonomy with a Dynamic Vehicle Model," *IEEE Transactions on Intelligent Transportation Systems*, vol. 19, no. 9, pp. 2994–3008, 2018.
 - [16] S. Sapia, A. Schimpe, and L. Ferranti, "Active Safety System for Semi-Autonomous Teleoperated Vehicles," in *2021 IEEE Intelligent Vehicles Symposium Workshops (IV Workshops)*. IEEE, 2021, pp. 141–147.
 - [17] B. Asadi and A. Vahidi, "Predictive Cruise Control: Utilizing Upcoming Traffic Signal Information for Improving Fuel Economy and Reducing Trip Time," *IEEE Transactions on Control Systems Technology*, vol. 19, no. 3, pp. 707–714, 2011.
 - [18] H. Chu, L. Guo, B. Gao, H. Chen, N. Bian, and J. Zhou, "Predictive Cruise Control Using High-Definition Map and Real Vehicle Implementation," *IEEE Transactions on Vehicular Technology*, vol. 67, no. 12, pp. 11 377–11 389, 2018.
 - [19] M. Althoff, S. Maierhofer, and C. Pek, "Provably-Correct and Comfortable Adaptive Cruise Control," *IEEE Transactions on Intelligent Vehicles*, vol. 6, no. 1, pp. 159–174, 2021.
 - [20] S. Magdici and M. Althoff, "Adaptive Cruise Control with Safety Guarantees for Autonomous Vehicles," *IFAC-PapersOnLine*, vol. 50, no. 1, pp. 5774–5781, 2017.
 - [21] B. van Arem, C. J. G. van Driel, and R. Visser, "The Impact of Cooperative Adaptive Cruise Control on Traffic-Flow Characteristics," *IEEE Transactions on Intelligent Transportation Systems*, vol. 7, no. 4, pp. 429–436, 2006.
 - [22] D. Schitz, G. Graf, D. Rieth, and H. Aschemann, "Model-Predictive Cruise Control for Direct Teleoperated Driving Tasks," in *2021 European Control Conference (ECC)*. IEEE, 2021, pp. 1808–1813.
 - [23] R. Rajamani, *Vehicle Dynamics and Control*, ser. Mechanical Engineering Series. Boston, MA: Springer US, 2012.
 - [24] A. Schimpe, J. Feiler, S. Hoffmann, D. Majstorovic, and F. Diermeyer, "Open Source Software for Teleoperated Driving," in *2022 International Conference on Connected Vehicle and Expo (ICCVE)*. IEEE, 2022, pp. 1–6.
 - [25] K. Burnett, A. Schimpe, S. Samavi, M. Gridseth, C. W. Liu, Q. Li, Z. Kroeze, and A. P. Schoellig, "Building a Winning Self-Driving Car in Six Months," in *2019 International Conference on Robotics and Automation (ICRA)*. IEEE, 2019, pp. 9583–9589.
 - [26] R. Verschuere, G. Frison, D. Kouzoupis, J. Frey, N. van Duijkeren, A. Zanelli, B. Novoselnik, T. Albin, R. Quirynen, and M. Diehl, "Acados-a Modular Open-Source Framework for Fast Embedded Optimal Control," *Mathematical Programming Computation*, 2021.
 - [27] G. Frison and M. Diehl, "HPIPM: a high-performance quadratic programming framework for model predictive control," *IFAC-PapersOnLine*, vol. 53, no. 2, pp. 6563–6569, 2020.
 - [28] M. O'Kelly, V. Sukhil, H. Abbas, J. Harkins, C. Kao, Y. V. Pant, R. Mangharam, D. Agarwal, M. Behl, P. Burgio, and M. Bertogna, "F1/10: An Open-Source Autonomous Cyber-Physical Platform," 2019. [Online]. Available: <https://arxiv.org/abs/1901.08567>